

Preliminary Thrust Characterization of the T-Series Hollow Cathodes for All-Electric Spacecraft

IEPC-2007- 81

*Presented at the 30th International Electric Propulsion Conference, Florence, Italy
September 17-20, 2007*

Angelo N. Grubisic* and Stephen B. Gabriel,†
Astronautics Research Group, University of Southampton, Southampton, SO17 1BJ, United Kingdom

David G. Fearn‡
Electric Propulsion Solutions, Fleet, Hants, GU14 0LX, United Kingdom

Abstract: This paper characterizes thrust performance of the T5 hollow cathode and a variant of the T6 hollow cathode modified for improved operational characteristics. Both forms of device display impressive propulsive performance and bring to light the potential for application as microthrusters. The T5 hollow cathode is shown to work in an almost purely electrothermal heating mode generating specific impulse as high as 427s with argon while operating below 100W. The variant on the T6 cathode is able to produce specific impulse of over 1050s with xenon and argon; however the acceleration mechanism at this performance is shown to be almost entirely electromagnetic effectively constituting a low power magneto-plasma-dynamic thruster. The T6 cathode also displayed very low discharge voltages ~12V and stable operation while carrying currents of 30-Amps and flow rates of less than 0.1mgs⁻¹ down to a minimum of 0.04mgs⁻¹ with xenon. This investigation highlights the importance of anode/keeper geometry in hollow cathode thruster design and indeed in all space based applications of hollow cathode.

Nomenclature

α	=	Degree of ionization
A	=	Area, m ²
amu	=	Atomic mass unit
C_p	=	Specific heat capacity, kJ/kg.K
d	=	Diameter, m
ε_i	=	Ionization potential, eV
e	=	Electron charge, C
E	=	Electric field, V/m
f	=	View factor
I	=	Current, A
J	=	Current density, A/m ²
k	=	Boltzman's constant, 1.381×10^{-23} J/K
L	=	Characteristic length, m
m	=	Particle mass, kg

* Doctoral Researcher, Astronautics Department, A.Grubisic@soton.ac.uk

† Head of Astronautics, Astronautics Department, SBG2@soton.ac.uk

‡ Sole Proprietor, Electric Propulsion Solutions

\dot{m}	=	Mass flow rate, kg/s
n	=	Particle density, m^{-3}
p	=	Internal cathode pressure, N/m^2
P	=	Power, W
q_r	=	Radiative heat flux, W
r	=	Radius, m
R	=	Resistance, Ohms
T	=	Temperature, K
μ	=	Magnetic permeability
V	=	Potential, V
η	=	Plasma resistivity, Ohm/m
λ_d	=	Debye length, m
$\ln A$	=	Coulomb logarithm
V_p	=	Plasma potential, V
v	=	Velocity, m/s
σ	=	Electrical conductivity, Ohms/m
γ	=	Ratio of specific heats (5/3 for xenon)

Subscripts

A	=	Anode
n	=	Neutrals
c	=	Cathode
D	=	Discharge current
d	=	Debye
$ds1,2$	=	Double sheath at orifice entrance and exit
e	=	Electrons
eq	=	Equivalent
ex	=	Exit
eff	=	Effective
em	=	Emitter
f	=	Fall
i	=	Ions
k	=	Keeper
oh	=	Ohmic
o	=	Orifice
s	=	Static

I. Introduction

THIS paper provides a characterization of the T5 and T6 hollow cathode performance in the role of standalone microthrusters. These particular cathodes are a mature technology developed extensively over the last 35-years for application on the UK-10, UK-25, T5 and T6 gridded ion thrusters^{1 2 3 4 5 6} and as an electron source for various ion beam neutralization applications.⁷ Previous testing at the University of Southampton on the T6 hollow cathode has shown that at least a basic thruster can be formed, generating moderate specific impulse (<300s with xenon) at thrust levels <2 milli-Newtons, however no attempt was made to optimize the device for improved performance.^{8 9}

Hollow cathodes may represent an attractive propulsion device for a number of reasons. Spacecraft which operate primary electrostatic or electromagnetic propulsion systems such as gridded ion thrusters and Hall thrusters are typically required to carry a secondary chemical system for reaction/momentum control or to compensate for thrust misalignment.^{11 12 13 14} These secondary systems constitute a large fraction of the overall propulsion system

mass which electric propulsion was originally designed to negate and brings substantial cost increases in manufacture, assembly, integration and test operations, and launch preparation.¹⁵ A simpler solution would be to use a moderate performance secondary system able to operate from a common propellant with the primary system; however the high molecular mass of xenon limits the performance of cold gas thrusters and resistojets to between 15-48s specific impulse.^{16 17} If hollow cathodes can be optimized as thrusters and show better performance, they may be well suited to this purpose. Concurrent design studies as part of this work, have highlighted the possibility of producing an all-electric lunar transfer orbiter utilizing the T5 gridded ion thruster and 8 hollow cathode AOCS thrusters at less than 150kg wet mass.¹⁸ A similar NEO rendezvous mission study utilizing 3 microsattellites with T5 gridded ion thrusters and T6 hollow cathode thrusters also generated relatively low-cost spacecraft (50 M€ for the first and 30 M€ for subsequent spacecraft) with a wet mass of less than 120kg.¹⁹

The low operating power of hollow cathode such as the T5 (<90W) may also present a microthruster suitable for smaller satellites (<150kg). Guidelines issued by the Inter-Agency Space Debris Coordination Committee (IADC) recommend that spacecraft in low earth orbit have the ability to deorbit within 25-years. This increases the mission delta-V by some 100-500% for typical earth observation missions.²⁰ As demands on small spacecraft also continue to grow for missions such as formation-flying, inspection and rendezvous, requiring drag compensation, constellation phasing and proximity maneuvering,²¹ conventional robust microsattelite propulsion systems such as cold gas thrusters and resistojets are deficient in performance. Microsattelite platforms however lack the resources to support advanced enabling technologies such as micro-ion engines and Hall thrusters. The diffuse arc in the T5 hollow cathode in particular permits operation at convenient discharge voltages (10-25V) for satellites with limited power electronics, especially when compared to other electrothermal, electrostatic or electromagnetic thrusters.²² Furthermore a hollow cathode microthrusters system would able to draw from existing inert propellant storage and feed architectures for conventional cold gas/resistojet systems which find considerable use on small satellites due to their simplicity and low cost nature. This makes their addition a reasonably simple process. The inert propellant also bares no contamination risk to sensitive spacecraft equipment when compared with other thrusters in the milli-Newton thrust range such as PPT's (Pulsed Plasma Thrusters), colloid and FEPP (Field Emission Electric Propulsion) thrusters.²³ Hollow cathode thrusters may therefore be a fitting compromise.

II. Cathode Operation and Analytical Description

This section discusses the T5 and T6 cathodes used in their respective thrust characterization and presents an analytical description of hollow cathode operation. A summary of the cathode specification is shown in Table 1 below.

Cathode Type	T5 STRV-A1 (1994)	T6 Discharge cathode
Maximum current [A]	0.5 - 3.6 @ 15,000hrs	1 - 15 @ 15,000 Extended at 30A
Flow range [mg/s]	0.03 to 1.2	0.1 - 3
Weight [g]	60	120
Operating Power [W]	<90	<1000
Orifice diameter [mm]	0.23	1
Orifice length [mm]	1	2 (50% chamfer)
Tip material	Molybdenum	Tantalum

Table 1 Summary of operating parameters and physical characteristics of the T5 and T6 cathodes used in this thrust characterization

A. T5 Cathode

The cathode characterized in this experiment is the T5 STRV-A1 (Space Technology Research Vehicle) DRA (Defense Research Agency) flight-spare launched in June 1994. This included an experiment to allow the hollow cathode assembly to demonstrate spacecraft electrostatic discharging.²⁴ The cathode is rated at a maximum DC

current of 3.2A at flow rates typically $0.04 - 1\text{mg s}^{-1}$ operating below 90W and is essentially standard. The T5 cathode was originally designed for the main discharge cathode in the UK-10 ion engine and has been extensively characterized.²⁵ The cathode contains a tungsten dispenser, 1.0mm i.d. x 2.8mm o.d. x 11mm, impregnated with a mixture of barium-oxide, calcium oxide and aluminates ($\text{BaO}:\text{CaO}:\text{Al}_2\text{O}_3$), which lowers the insert's work function for thermionic emission, and maintains a working temperature of $\sim 1000^\circ\text{C}$. At maximum rated current capacity, the T5 dispenser emits with a current density of at least $400\text{A}\cdot\text{cm}^{-2}$. A solid molybdenum tip welded to the cathode body contains an axial orifice 0.23mm in diameter and 1mm long. The T5 cathode is shown in Figure 1.

The open keeper has a 3mm diameter aperture and is mounted 3mm downstream of the cathode tip with the whole assembly mounted on a UK-25 ion thruster back-plate. In typical hollow cathodes a keeper electrode usually draws approximately 1-Amp of current, however in this study the cathode is operated in an open-diode configuration with the full discharge current being drawn to the keeper, which is now termed the anode. Previous studies on this type of hollow cathode have incorporated a much larger anode disk and a secondary discharge between the keeper and the anode and also an applied magnetic field to simulate a Kaufman ion engine environment. Open-diode configuration is more representative of a standalone microthruster configuration with no need for a coupled discharge. The T5 HCT is shown in Figure 1a and 1b.

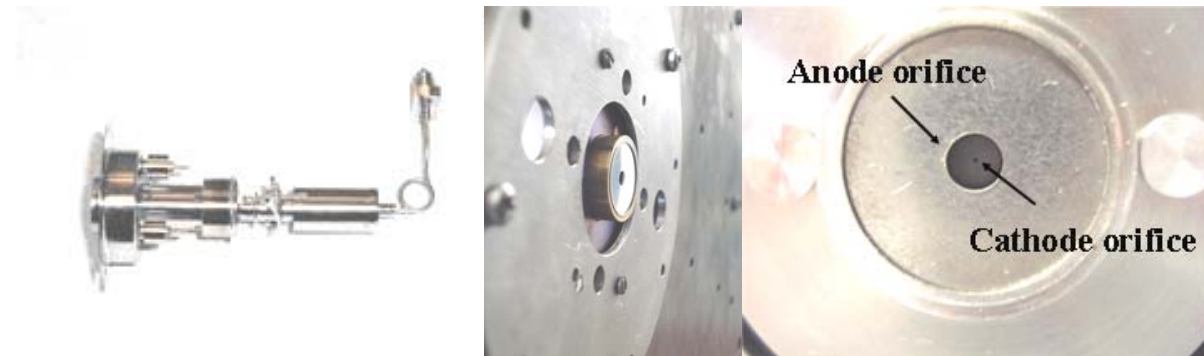


Figure 1a T5 Hollow Cathode Assembly, Figure 1b T5 mounted to UK-25 back plate, and Figure 1c T5 face

B. T6 Cathode

T6 Hollow Cathode used in this experiment is derived from neutralizer of the ROS-2000 HET (Hall Effect Thruster) developed by QinetiQ for Astrium under contract to ESA and is shown in Figure 2. The cathode is rated to a maximum of 30-Amps with extended operation up to 50-Amps with flow rates ranging from 0.1-3mg/s, typically operating at a few hundred watts. The tungsten dispenser is 2mm i.d. x 5mm o.d. x 10mm, with an emissions area over seven times that of the T5, while maintaining current densities of at least $1500\text{A}\cdot\text{cm}^{-2}$ at maximum rated current capacity. The cathode is constructed from a solid tantalum piece with a 1mm axial orifice through a 2mm thick orifice plate with a 45° chamfer at the exit to a depth of 1mm leaving an orifice of 1mm length. In this case the T6 anode and support housing has been specially designed to maximize available anode-plasma contact area on the basis that this parameter has a strong influence on the minimum attainable flow rate and in reducing the discharge voltage (discussed more fully in the next section). The T6 cathode is mounted to a ceramic insulator which also connects to the anode housing. A 25mm diameter 30° conical diverging nozzle constructed from graphite with a 4mm orifice at the upstream end is mounted 0.5mm in front of the cathode and axially aligned. All flanges are sealed with grafoil gaskets. The T6 thruster is shown in Figure 3.



Figure 2 T6 ROS-2000 HET Neutralizers

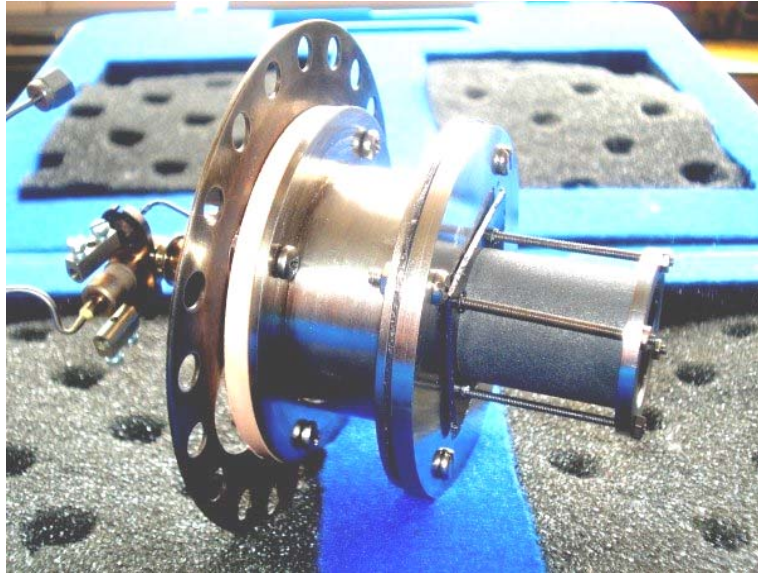


Figure 3 T6 hollow cathode thruster with modified anode and housing

C. Ignition and Operation

An internal cutaway of a T5 cathode is shown in Figure 4 which is at least functionally comparable to the T6. A tungsten heater is used to raise the temperature of the emitter ($>1000^{\circ}\text{C}$) sufficient for initial thermionic emission. A trigger voltage applied to an external electrode is typically used to initiate the discharge (15-200V). The orifice plate increases the internal pressure and generates sufficiently dense plasma within the internal volume to promote ion recombination at the emitter surface. Self-heating is then maintained by the acceleration of ions through the sheath (region between the cathode and plasma column), which recombine on internal surfaces to form neutrals. Confining the plasma column within the hollow cavity of the cathode permits operation at low cathode fall voltages while allowing high currents to be carried.

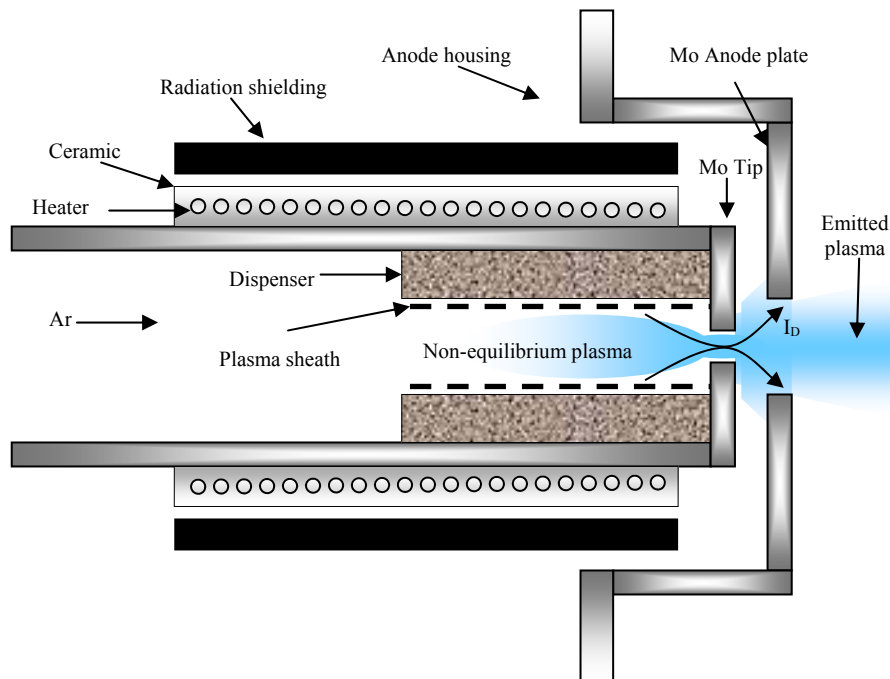


Figure 4 Internal schematic of a T5 cathode

The plasma column induces sheath-enhanced emission at the emitter surface due to the intense field ($\sim 10^7$ V/m) between the plasma column and cathode potentials at a distance on the order of the Debye length. These impregnate constituents undergo thermo-chemical reactions and liberate free Ba/BaO/CaO, which are adsorbed from the emitting surface during heating and operation. These components introduce a dipole and decrease the electronegativity barrier of the emitting surface, corresponding to a decrease in work function for thermionic emission.²⁶ Emitter life is generally based on the ability of the emitter to liberate free barium, where the rate of desorption is considered temperature dependant and a function of the emitted current density.

Thermionically emitted electrons are accelerated through the sheath potential and considered as a mono-energetic beam. The plasma potential within the emitter volume generally remains 8-10V above the cathode potential (however lower values are recorded in large orifice cathodes) consistent with the energy required for the excitation of meta-stable states of xenon ($3P_0 \sim 9.45$ eV, $3P_2 \sim 8.32$ eV). Ion production is generally assumed to be achieved by multi-step processes firstly by electron impact of primary electrons from the atomic ground state²⁷ within the emitter volume, and then by lower energy thermalized electrons (2-4eV) within the orifice which then contribute significantly to the ionization process. The total process thus requires transfer of at least the ionization energy (12.13eV for xenon). The discharge current is drawn through the orifice toward the anode. Processes within the orifice dominate performance. The operating regime acts to maintain emitter temperatures for thermionic emission by balancing power deposition to the cathode with cooling by particle efflux and heat transfer to the surroundings.

Energy input to the plasma can be attributed to the energy of thermionically emitted electrons accelerated through the cathode fall and through Ohmic (collisional) heating within the orifice channel. While direct measurements have not fully characterized the processes following ignition, it is considered that xenon plasma initially forms between the orifice plate and the anode. This plasma extends into the hollow core of the cathode insert. Coupling of the electric field into this region drives the ionization electrons that ultimately provide the breakdown of the main discharge. Since Ohmic heating of the plasma volume within the emitter is small compared to the orifice due to relative number densities in the respective volumes, orifice geometry drives resistive dissipation and energy equipartition to the plasma. This may have a strong influence on an electrothermal thruster's performance. In the T5 cathode an ionization fraction close to 1 has been found at the orifice exit²⁸ in comparison to other ion engine applications where gas utilization is typically low (5-10%). The T5 orifice diameter is 25% that of the T6. This would suggest the T5 cathode may be a good candidate for operation at lower powers, but with relatively high specific powers (J/mgs^{-1}) as an electrothermal thruster.

D. Spot and Plume Modes

Spot and plume-modes are the two major discharge regimes considered in orificed hollow cathode design, especially important when operating off a small satellite bus at low powers. If the flux of ions into the cathode-anode gap is sufficient, the anode will passively collect the discharge current from the plasma. This type of operation is referred to as spot mode. If the ion flux to the cathode-keeper gap is not sufficient for the anode to passively collect the electron current, an additional voltage drop forms between the plasma and anode to facilitate ionization so that electrons can traverse the gap within the quasi-neutral plasma. This occurs as the mass flow rate or discharge current is decreased beyond a critical point, and is termed plume mode. Since in plume mode the ions created in the gap have some fraction of the cathode fall to accelerate them toward the cathode orifice plate, it exhibits ion sputtering²⁹ and discharge instabilities, which limit lifetime³⁰ and give high coupling voltages. As in cathode development for ion engines, consideration must be given to maintain reasonable discharge voltages and operating temperatures for adequate lifetime. This is normally limited by impregnate depletion in Kaufman type ion engines and ion sputtering in ring-cusp chamber designs. Application as an electrothermal thruster will demand high current densities within the orifice to maximize Ohmic heating therefore the maximum tolerable tip temperature for adequate thruster life will dictate the limiting current density and maximum acceptable power deposition into the orifice. Operation at orifice plate temperatures below 1300°C has typically been used in development of low power low flow 3.2mm cathodes consistent with practices proven to enable lifetimes greater than 10,000 hr.³¹

E. Energy Balance

At the hollow cathode surface the dominant energy gain processes are thermal energy input by ion bombardment and hot plasma electrons with energies sufficient to exceed the cathode fall voltage, while energy is lost by convective cooling, thermionic emission and radiative flux. This power balance is represented by:

$$\int J_{th} \left(\phi_{eff} + \frac{5kT_e}{2e} \right) dA_e = \int J_i (\varepsilon_i + V_f - \phi_{eff}) dA_e + \int J_e \left(\phi_{eff} + \frac{5kT_e}{2e} \right) dA_e - fq_r \quad (1)$$

With a view factor from the emitter to the cathode body:

$$f = \frac{A_e}{A_s} \quad (2)$$

The power delivered by the ions consists of the kinetic energy of the impact and the energy released when the ion recombines. The energy of the thermionic electrons can be approximated as a mono-energetic beam since the energy gained by acceleration through the sheath is much greater than the thermal energy, and assumes a collisionless sheath. In this analysis it is assumed that energy deposited into the cathode surfaces other than the emitter does not return to the plasma except as radiation and heating of cold neutral atoms.

F. Plasma Power Balance

Since the emitter temperature profile is not constant along the length of the cathode^{32 33}, integrals allow for the resulting variation in current density from the emitter. Electron emission provides energy to the plasma in the form of electrons accelerated by the cathode fall. This energy is utilized to ionize and excite the gas, and heat the plasma electrons. Energy is also added to the plasma by Ohmic heating of the resistive plasma within the orifice. Energy is lost by particles flowing out of the cathode, given by:

$$\int J_{th} \left(V_p + \frac{5kT_e}{2e} \right) dA_{em} + \int \frac{J_D^2}{\sigma} dV = \int J_i \left(\varepsilon_i + \frac{5kT_i}{2e} \right) dA_s + \int J_e \left(\frac{5kT_e}{2e} \right) dA_s + (I_D + \alpha I_{eq}) \left(\frac{5kT_e}{2e} \right) + \frac{I_{eq}}{\alpha} \left(\frac{5kT_e}{2e} \right) + q_r \quad (3)$$

Where equivalent flow rate is defined by:

$$I_{eq} = \frac{e\dot{m}}{m_i} \quad (4)$$

If the configuration of the thruster allows for the condition of fully ionized plasma at the orifice exit with a high degree of gas utilization, then the energy balance can be expressed as:

$$I_{th} \left(V_p + \frac{5kT_e}{2e} \right) + \int \frac{I_D^2}{\sigma} dV_{oh} = I_i \left(\varepsilon_i + \frac{5kT_i}{2e} \right) + I_e \left(\frac{5kT_e}{2e} \right) + (I_D + I_{eq}) \left(\frac{5kT_e}{2e} \right) + I_{eq} \left(\frac{5kT_e}{2e} \right) + q_r \quad (5)$$

This assumes Ohmic heating of the plasma volume within the emitter is small compared to the orifice due to relative number densities in the respective volumes.

G. Discharge Parameters

The total discharge current is based on the contributions of all particle fluxes at the cathode surface for preservation of current continuity and is expressed as:

$$I_D = I_{th} + I_i - I_e \quad (6)$$

The total discharge voltage can be expressed as:

$$V_d = V_p + \Delta V_{ds1} + \Delta V_{oh} + \Delta V_{ds2} \quad (7)$$

This is the sum of the cathode fall voltage, the Ohmic drop across the orifice and the double sheaths at the entrance and exit of the orifice.

H. Energy Conservation

At the insert surface, the energy loss due to convected thermionic electrons is balanced primarily by ion bombardment. If energy input due to plasma electrons overcoming the fall voltage is neglected (since the fall voltage is much greater than most of the electron energies for a Maxwellian distribution) the energy balance can be expressed as:

$$\int J_{th} \left(\phi_{eff} + \frac{5kT_c}{2e} \right) dA_e = \int J_i (\varepsilon_i + V_f - \phi_{eff}) dA_e \quad (8)$$

The working temperature of a given emitter is therefore a product of the fall voltage, particle densities and emitter geometry for sustained thermionic emission.

I. Plume Mode Transition

To ensure the cathode consistently operates in spot mode the thermal flux of electrons to the anode must be at least be equal to the discharge current. An empirical transition to spot mode criterion³⁴ has been described by Kaufman, which accurately predicted the transition flow rate. Katz has numerically determined this transition on the basis of the contact area of the anode with the downstream plasma. The necessary surface area of anode is calculated by the thermal flux of electrons to the surface, given by:

$$\frac{I_D}{I_A} = \frac{I_D}{I_i} \left(\frac{d_{AK}^2}{A_A} \right) 4\pi^{3/2} \sqrt{\frac{m_e T_i}{m_e T_e}} \quad (9)$$

where the plasma density is determined from the proportion of the ion output from the orifice, which is in contact with the anode surface.

Dimensions of the anode aperture in the T6 anode design were selected to allow for at least 50-Amps of discharge current to be collected for testing purposes even with gas utilization as low as 10% since the high utilization assumption may not be reflected in experiment. A thermal model of the T6 cathode thruster assembly is shown in Figure 5. This was used in the thermal design and hence graphite was selected for the anode nozzle due to the heat deposited primarily by convective electron cooling during operation.

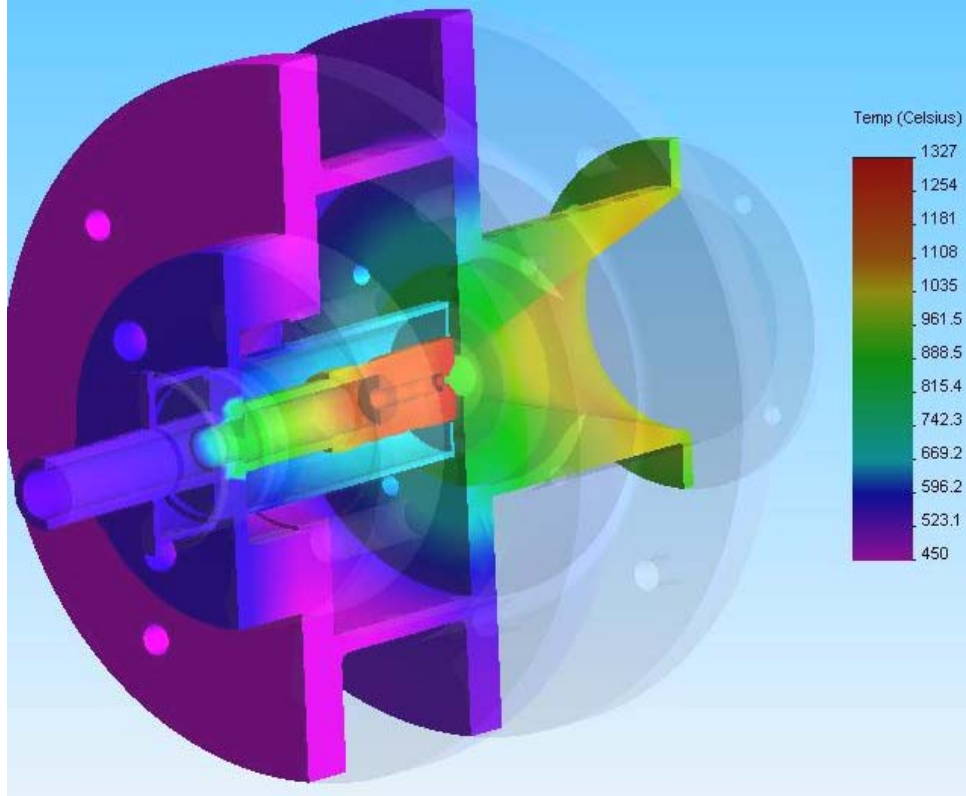


Figure 5 T6 Hollow cathode thruster assembly thermal model operating at 30A with argon on 0.05mgs⁻¹

III. Thrust production

Plasma models suggest that cathodes are capable of generating peak heavy particle temperatures greater than 6,000K with wall temperature not exceeding 1,500K.³⁵ Laser Induced Fluorescence (LIF) has identified neutral temperatures in cathode-keeper gaps are between 1800-4000K, well above cathode wall temperature.³⁶ Experiment has also suggested heavy particle temperatures between 3200-6000K necessary to explain elevated backpressures within conventional cathodes.³⁷ Assuming the plasma and remaining neutrals undergo some degree of adiabatic expansion it is reasonable to assume some level of thermal energy conversion to directed kinetic energy of the flow which is dependant on the plasma heating modes. The main mechanism of plasma heating is known to be Ohmic heating by plasma electrons within the cathode orifice with collisional heat transfer to the heavy particles.³⁸ A thermal thrust mechanism with significant arc heating within the cathode would be possible while low wall temperatures are maintained (<1700K) given the low plasma densities contacting the orifice ($\sim 10^{20}/m^3$)³⁹ The electron temperature within the orifice is typically 11,600-23,200K (1-2eV), depending on the degree of Ohmic heating. The performance of any electrothermal device can be approximated by means of a rudimentary one-dimensional energy argument that limits the exhaust speed of the flow from a fully expanded nozzle to:

$$v_{ex} \leq \sqrt{C_p T_{prop}} \quad (10)$$

When considering thermalization of the propellant to produce thrust with xenon, krypton or argon, the theoretical limit to specific impulse (assuming full conversion of thermal to directed kinetic energy) is shown in Figure 6.

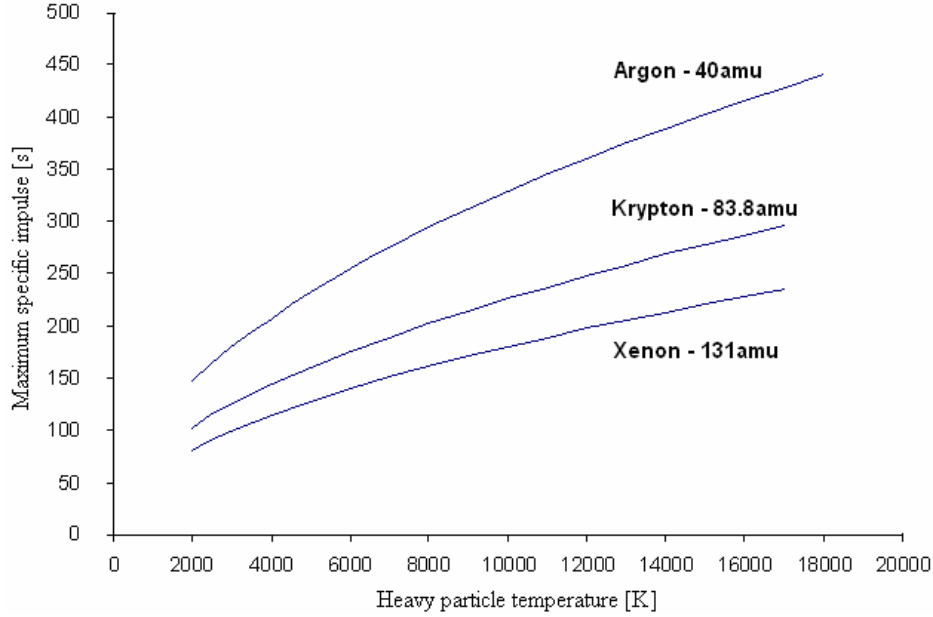


Figure 6 Limiting specific impulse for purely thermalized propellants based on full energy conversion

Accounting for the specific impulse found from the T6 even in early testing requires heavy particle temperatures too high to be described by a thermal thrust mechanism alone. The T6 may therefore experience a degree of electromagnetic acceleration of the charged particles by pinch forces in the plasma, which is reasonable at 25 Amps. The T5 cathode however operates at much lower currents and therefore is expected to operate in an almost purely electrothermal mode. Thrust production by magneto-plasma-dynamic forces, pressure and momentum thrust at the orifice exit can be estimated by assuming a blowing force acts on the plasma and by the various particle pressures at the orifice exit. Where, assuming that all particles behave like a perfect dilute gas, and neglecting magnetic pinch effects, the plasma pressure in the hollow cathode orifice can be evaluated from the equation of state:

$$p_{em} = n_e k T_e + n_i k T_i + n_n k T_n \quad (11)$$

Considering the small orifice area compared to the cross sectional area of the internal diameter of the cathode, the internal pressure may, as a first approximation, be estimated from the critical flow relation for sonic flow through the orifice, assumed to be adiabatic.

$$p_{ins} = p_{or} \left(1 + \frac{\gamma - 1}{2} \right)^{-1/(\gamma - 1)}$$

$$F_{thrust} = \dot{m} v_{ex} + p^* A_o \quad (12)$$

Assuming invicid flow, the theoretical thrust can be written as flow through a nozzle, the isentropic thrust given by:

$$F_{nozzle} = \left[\left(\frac{2}{\gamma - 1} \right) \left(\frac{2}{\gamma + 1} \right)^{\gamma + 1/\gamma - 1} \left(1 - \frac{p_{ex}}{p_s} \right) \right]^{0.5} p_s A_t + p_{ex} A_{ex} \quad (13)$$

In the case of a flat plate orifice with infinite expansion ratio, $\varepsilon = \frac{A_{ex}}{A_t} = \infty$ and $p_e = 0$,

the equation can be written as:

$$F_{orifice} = y \left[\left(\frac{2}{y-1} \right) \left(\frac{2}{y+1} \right)^{y+1/y-1} \right]^{0.5} p_s A_o \quad (14)$$

While this relationship may serve as a first approximation, deriving the internal pressure contributions of all internal particles is a far from easy task both theoretically and experimentally due to the inability to characterize the internal plasma parameters accurately. Assuming that a cathode is able to operate at very low flow rates where the degree of pressure contribution may be assumed negligible, it can be shown that MPD acceleration forces become increasingly dominant. A stream wise acceleration is provided by the crossing of the radial arc current with the self generated azimuthal magnetic field through the cathode orifice, an essentially scalar crossed-field interaction given by:

$$F_z = \frac{\mu J^2}{4\pi} \left(\ln \frac{r_a}{r_c} + \frac{1}{4} \right) \quad (15)$$

Assuming the current density through the orifice is uniform, a virtual cathode radius can be set to the orifice diameter. The theoretical specific impulse arising from the blowing component when operating the given T6 setup described earlier at 30, 20 and 10 Amps for any given propellant can be estimated. Theoretical specific impulse arising from the blowing force at any propellant mass flow rate is shown in Figure 7.

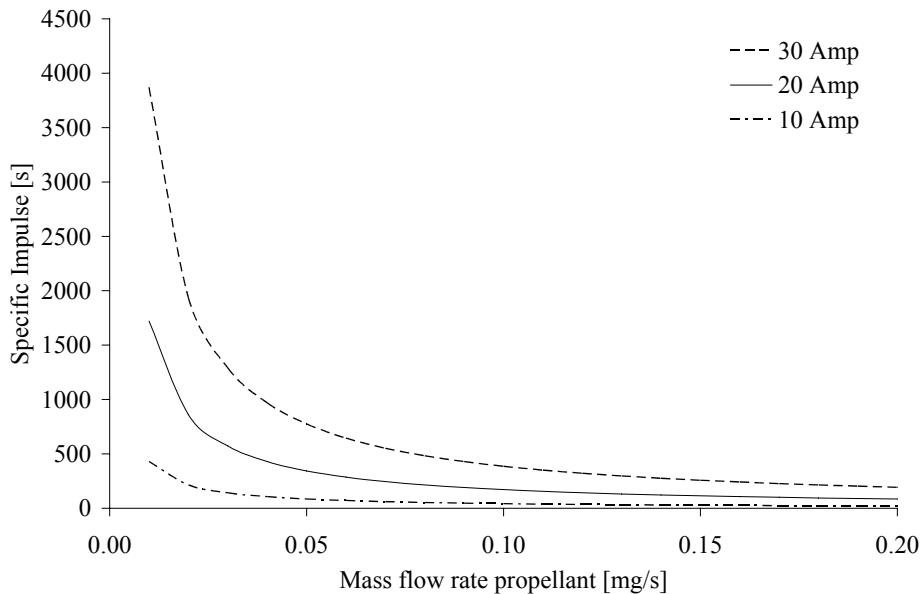


Figure 7 Theoretical specific impulse as a result of blowing force from the given T6 high current hollow cathode setup

One would be inclined to think that the total blowing force would be much smaller since there also exists a counterproductive blowing force at the orifice entrance (from the movement of the electron current from the insert towards the constricted orifice) which is only loosely dependant on geometry and must therefore be similar to the thrusting force. However the counter blowing force merely causes an artificial backpressure buildup within the internal cavity of the cathode which reaches equilibrium with the counter-blowing force to maintain a constant mass flow rate. This internal blowing force, while being important in establishing the internal operating parameters of the cathode, especially at low mass flow rate, can be neglected in the thrust production process.

Assuming two cathodes of equal orifice and anode diameters to the T5 and modified T6 cathodes (0.25mm, 3mm and 1mm, 25mm respectively) theoretical thrusts for blowing force are shown in Figure 8. It should be noted that the discharge currents considered here are well in excess of the rated operating currents for the T5 cathode however it does show the significance of geometry in production of the blowing force.

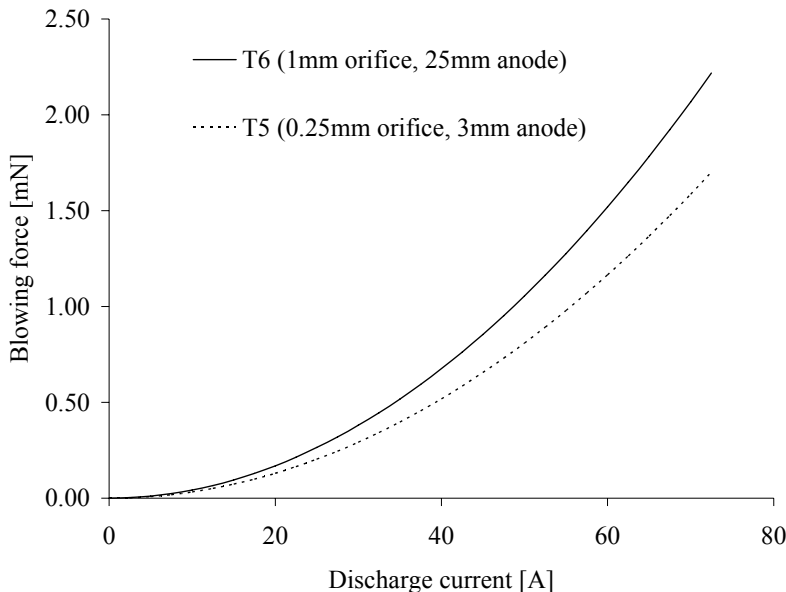


Figure 8 Blowing force with discharge current for two configurations of hollow cathode

IV. Experimental Setup

A. Vacuum Rig

The vacuum rig used in this experiment is described in ⁴⁰ previously used for hollow cathode characterization within the UK-25 ion engine. The rig consists of a 500mm diameter by 500mm long chamber with ISO and CF flanges. Three main ISO 160 ports allow connection of the pumping system with viewports on either side of the vacuum chamber allowing optical access. Four CF35 ports integrated into the ISO500 door flange allow feed-through access. Pressure gauge heads are located in KF25 and KF40 ports on top of the chamber. A cylindrical water cooled copper shroud fitted around the inside of the vacuum chamber wall is used to dissipate heat load with the water feed-through entering from a CF35 port at the blank end of the chamber.

Pumping is achieved with a water-cooled turbo molecular pump (Pfeiffer Balzers TPH 520KTG, 500l/s) controlled by a TCP 380 power supply (with a TCS303 pump control unit) and backed by a rotary vane pump (Edwards EH500A H/C 80 CMH), achieving an ultimate vacuum of 10^{-8} mbar. This level of vacuum ensures the partial pressure of oxygen in the system is low enough to prevent poisoning of the chemically sensitive thermionic emitter. Propulsion grade argon (99.997% pure) is passed through high and low capacity oxygen traps via an Edwards FCV10K extra fine control needle valve. Vacuum pressure is monitored with a Balzers TPG300 pressure gauge package constituting a pirani ($1000-5.4 \times 10^{-4}$ mbar) and cold cathode gauge head ($5 \times 10^{-3} - 1 \times 10^{-9}$ mbar). Prior to operation the cathode was allowed to outgas at a pressure $< 1 \times 10^{-6}$ mbar for 2-days. After this outgassing the heater was operated at a current of 0.5A for 24 hours. This ensured that the flame sprayed heater ceramic is well outgassed and therefore the chances of the heater failing are dramatically reduced.

The propellant supply system is designed to be flexible and accommodate a large range of flow rates for full thrust characterization of the T5 and T6 cathode. A Spectra Gasses 7120 high accuracy double-stage regulator supplies propellant to the feed system. A sampling cylinder (bypassed during experiment) and Druck PDCR910

pressure transducer are used for flow calibration before each round of testing with a repeatability of better than 4%. All external feed lines are above atmosphere pressure to reduce the possibility of air leaks into the flow system.

B. Power Supplies

The typical T5 gridded ion thruster from which the T5 hollow cathode is derived comprises nine independent supply units to power various elements of the system. In operation of the T5 and T6 cathode as a stand-alone thruster, the number of power supplies is reduced to three. It is also worth noting that since the cathode is in effect self-neutralizing, there is no need to electrically float the thruster system to a high positive potential, removing the requirement for electrical isolation of the thruster mounts and propellant feed lines. The electrical wiring system inside the chamber is also designed to minimize the influence of any MHD effects on the plasma both within the cathode and on the externally emitted plasma which may influence the thrust vector.

The power supply system used to operate the T5 hollow cathode is shown schematically in Figure 9. The cathode heater supply (Powerbox Lab605) provides the 2.2A required to heat the cathode to ignition temperatures ($>1000^{\circ}\text{C}$) prior to discharge ignition. The heater supply is operated in constant current mode with a common ground to the cathode potential to minimize the voltage difference between the heater wire and cathode body, reducing the risk of heater insulation breakdown. The discharge power supply consists of a high voltage (1kV, 30mA) strike supply and a low voltage (80V, 37A) steady state supply protected by diodes.

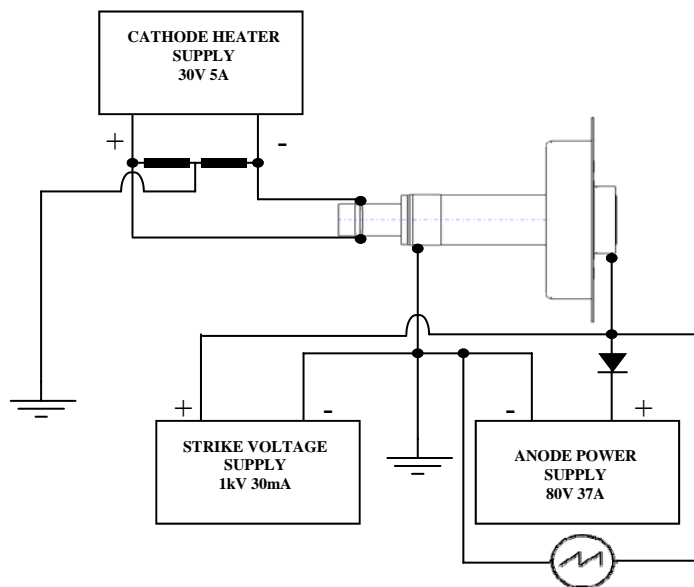


Figure 9 Electrical setup schematic

The strike voltage is supplied by a pair of Farnell Hivolt PM1/DCP photo-multiplier supplies connected in parallel and powered by a pair of Farnell 16RA24012 linear 24V power supplies. Once the discharge is initiated, steady state power is provided by a Glassman LV80-37 DC power supply. This is a 3kW switch mode supply with load regulation of $\pm 0.1\%$ and an output ripple of 10mV RMS over the frequency range 20Hz-20MHz. Plasma noise and instabilities in the discharge are monitored with a Gould 1600 digital oscilloscope connected across the anode power supply. Anode voltage current characteristics are monitored via the supply digital meters, limiting the resolution of the readings to $\pm 0.1\text{A}$ and $\pm 0.001\text{V}$, while strike voltage was monitored by a digital multi-meter with a resolution of $\pm 0.001\text{V}$.

C. Optical Thrust Measurement System

Optical setup consists of a Miles Grilot He-Ne (543.5nm) laser passed through a Keplerian beam expander and directed through the chamber onto a mirror, rigidly connected to a molybdenum pendulum target shown in Figure 10. The optics system guides the reflected beam out of the chamber and onto a Hamamatsu 4.7 x 4.7mm two-dimensional tetra-lateral photo-sensitive-detector (resolution of 600nm) at a path length of 0.86m. The detector is coupled with a C4674 signal processing circuit (output +/-2.5V at 1V/mm on each axis) is designed to provide two-dimensional position data on the incident light spot independent of the light intensity and is powered by a 30V Instec dual-tracking power supply (ripple less than 3mV). The output from the signal processing circuit is displayed on a Tektronix TDS 410A 2-channel digital oscilloscope (resolution +/-0.001V). A pivoting mechanism allows the target to be positioned both perpendicular to the thrust vector and through a full 90° sweep of angles, while also allowing the pendulum to be electrically floated, grounded or biased.

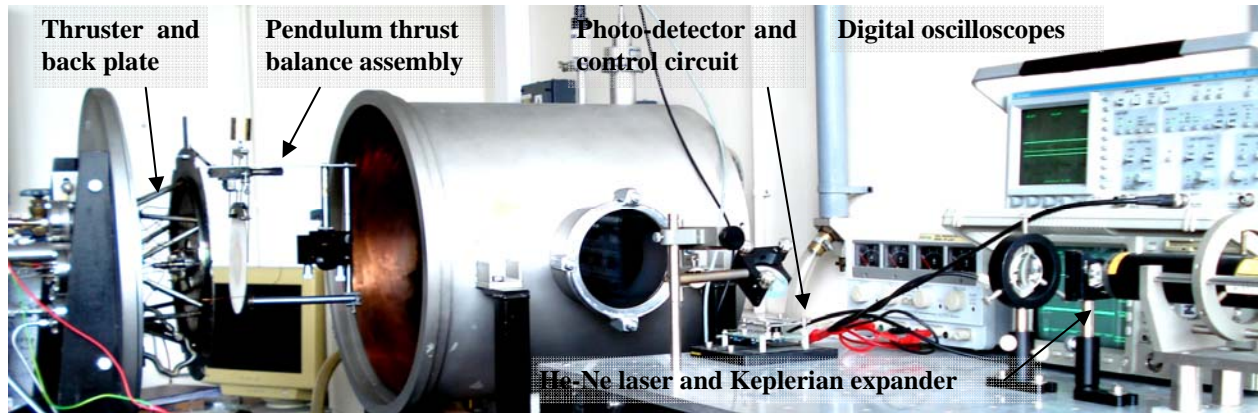


Figure 10 Experimental setup

The pendulum thrust balance, shown in Figures 10 and 11, is mounted on a beam fixed to the UK-25 ion thruster back plate and is positioned with the cathode on axis with the centre of the target.

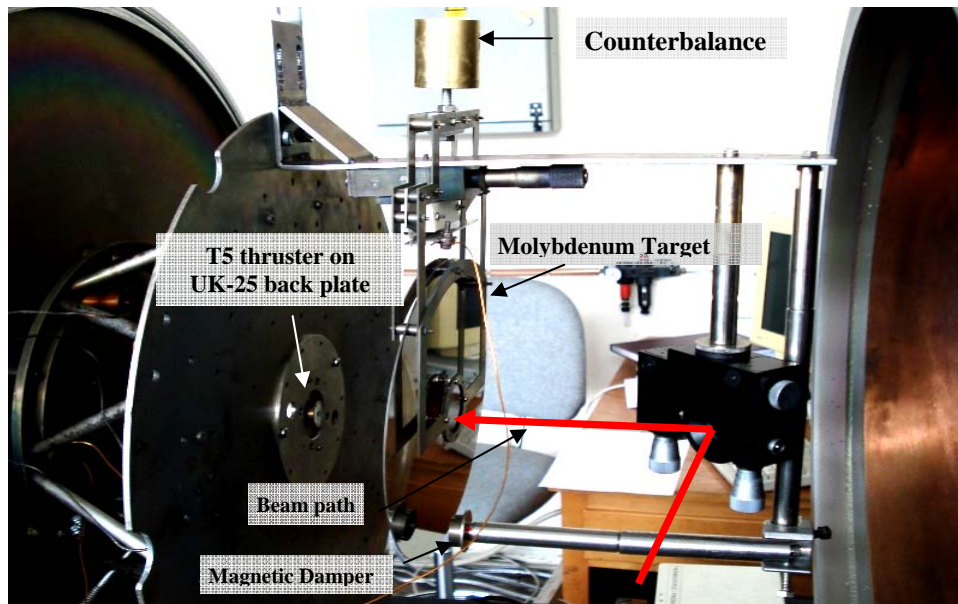


Figure 11 Pendulum thrust balance assembly

The stand-off distance between the pendulum target and the thruster can also be set between 20-250mm and micro-translation mechanism is used to finely adjust the position of the target. Unwanted oscillations in the system are passively damped by magnetic induction of a weak magnet placed close behind the Molybdenum target, electrically dissipating energy in the system. The optical detection setup of a green He-Ne laser mounted externally, two convex lenses forming a Keplerian beam expander and four mirrors.

V. Results and Discussion

A. Cold Gas and Resistojet Thrust Measurement

The hollow cathodes can be operated in a cold gas and resistojets mode (with the cathode heater only operating) in addition to the discharge mode. The system therefore allows for 2-levels of partial redundancy if the discharge is not able to ignite. Tests were conducted with argon for the T5 and with argon and xenon for the T6 cathode to characterize possible performance in these two modes and give some indication of the degree of elastic or non-elastic collisions with the target. Figures 12 and 13 show the thrust and specific impulse obtained when operating in a cold gas and resistojets mode. During the heated mode, the T5 cathode was operated at 19.7W heater power with the T6 operated at 50W.

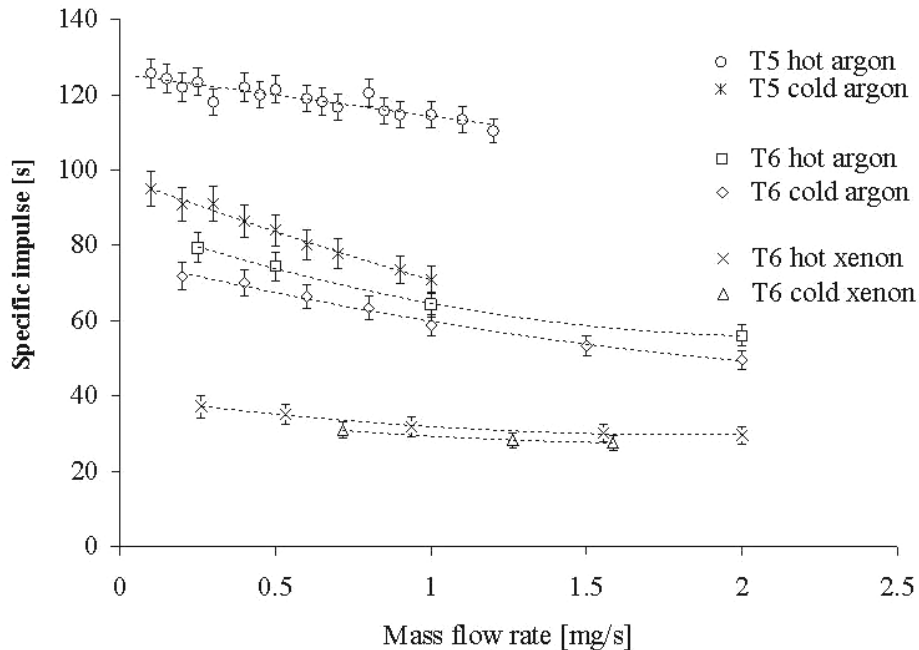


Figure 12 Specific impulse obtainable from operating the T5 (argon) and T6 cathode (argon and xenon) in a cold gas and resistojets mode (using only the heater)

The T5 thruster shows relatively high specific impulse with argon, surpassing the performance of the T6 in both modes of operation. Error bars are indicative of thrust measurement inaccuracies due to external excitations of the thrust balance, primarily from the roughing pump. Thrust measurements were made with good repeatability down to approximately 0.08mN, after which it became difficult to resolve thrust measurements with the sensitivity of the current balance setup.

The smaller orifice (0.23mm) of the T5 cathode is shown to be beneficial in thrust production for the same mass flow rate, since a higher chamber pressure is maintained and thus a greater thrust produced by the adiabatic expansion from the flat plate orifice. During the heated mode, higher internal pressure also allows a greater residence time for the propellant inside the cathode, improving heat transfer from the cathode walls by conduction.

This increase in heat transfer raises the chamber pressure further and thus produces a marked increase in performance over the cold gas mode, even more so when considering the respective heater powers. The T5 cathode achieved a maximum Isp of 125s at 0.12mN. This increase is much less pronounced in the T6 cathode due to the large orifice, chamber pressures therefore remain low and the resistojet mode only has a small influence on improving specific impulse. As expected operation with xenon in the T6 cathode leads to a large reduction in specific impulse due to the molecular weight of the gas, with a maximum Isp of 31.8s at 0.29mN obtained in resistojet mode. The loss of performance at higher mass flow rates is likely due to greater interaction between the expansion plume and the anode orifice edge and face. At the time of writing, T5 testing had not been conducted with xenon, however it is very likely that the T5 will also experience a reduction in performance scaling with the reduction found in the T6 cathode. This indicates that probable attainable Isp for the T5 cathode with xenon would be in the 50-60s range in resistojet mode.

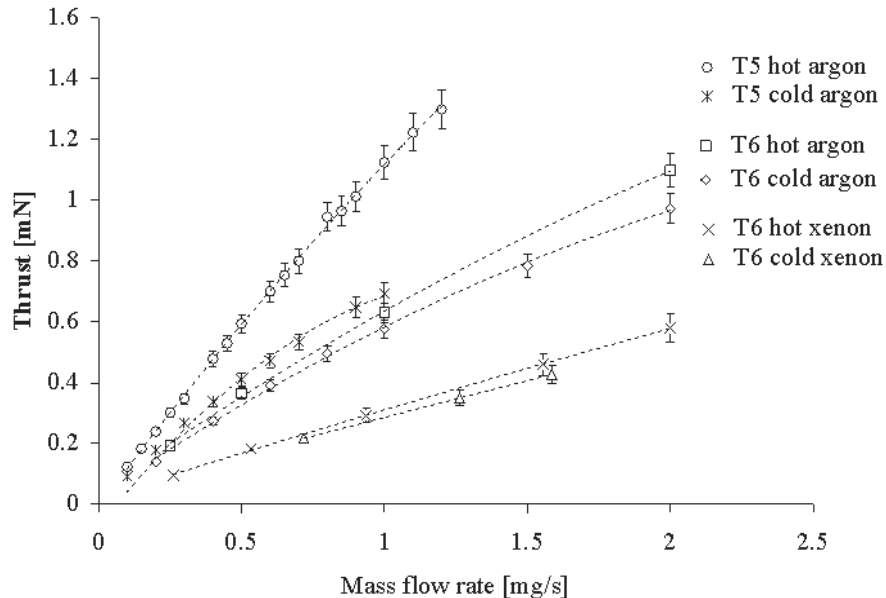


Figure 13 Specific impulse obtainable from operating the T5 (argon) and T6 cathode (argon and xenon) in a cold gas and resistojet mode (using only the heater)

B. Initiation of the Discharge

One factor important for operation in a discharge mode is the reaction time of the system. Since hollow cathodes require heating prior to ignition, this has to be taken into account when considering power budgets and the sequencing of thruster firings. Prior to ignition the T5 and T6 heaters were operated at 2.2A +/- 0.1A and 2.5A +/- 0.1A respectively for approximately 20 minutes to begin thermionic emission from the dispenser. Since power supplies were current limited, the heater voltage drop determined the input power. Figure 14 shows the results of 20 ignition characterization cases for the T5 and T6 cathodes, along with a typical heater power profile.

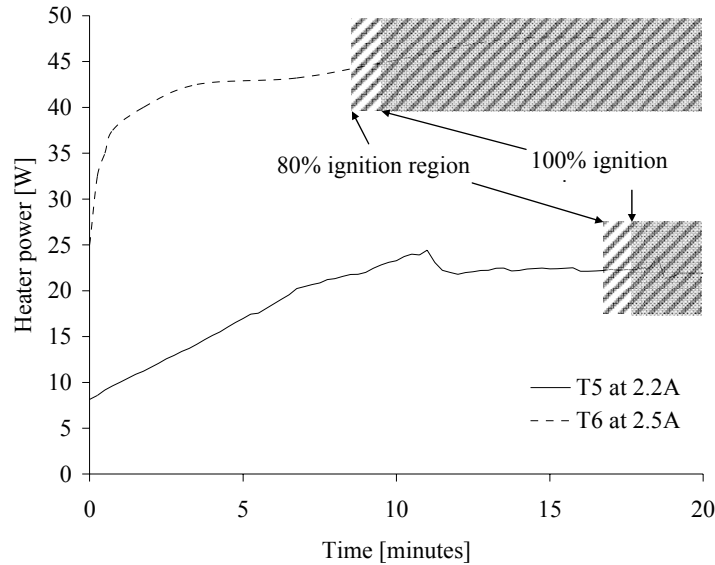


Figure 14 Heater input power over the pre-ignition heating period for the T5 and T6 cathode showing the times at which 80% and 100% of the test cases gained ignition

In the case of the T5 cathode voltage increases slowly during heat-up cycle since the heating element is firmly integrated into the cathode body, and therefore heater resistivity is subject to the thermal inertia of the assembly. Start-up time for the T5 is in the region of 17-minutes for 80% of cases and 18-minutes for the remaining 20%. Small fluctuations in heater power are due to thermal and electrical conductivity changes in isolated regions of the heater and insulation. The relatively large drop in heater power after 11-minutes of preheating is due to the increased radiative flux from the cathode assembly which in-turn lowers the resistivity and therefore the dissipative power of the heater. It is also worth noting that purging of the cathode with a gas flow during the preheating time also increases the start-up time in the T5 cathode by some minutes due to convective cooling slowing the assembly heat-up time. Early ignition was possible based on previous operation of the thruster raising the assembly temperature, particularly in the T5 case. After operating at high power >60W it was also found that reignition of the cathode was possible with out the heater voltage being applied up to a minute after switch-off due to the remnant temperature of the assembly. Operation at lower powers <15W however required almost the full preheating time to reignite due to the low power deposition into the assembly.

In the case of the T6 cathode, the heater is primarily radiative rather than conductive; therefore the voltage increases very rapidly at the start of the cycle. As the assembly heats up there is only a small increase in heater power due to the limited conductivity. The T6 cathode ignited readily at around 7.5 minutes, while all ignitions had occurred by approximately 9.5 minutes. The T6 cathode also does not experience the voltage fluctuations found in the T5 start-up cycle since the radiative heater reduces the possibility of hot spots forming.

C. Strike Voltage

Although a strike voltage was available to initiate electrical breakdown of both cathodes, the anode voltage (set at 70V) was always sufficient to initiate both discharges. In application as a thruster especially on small satellites the breakdown voltage is important due to limited power electronics resources, generally consisting of an unregulated 28V bus and regulated 5V bus. In an attempt to quantify the maximum operating voltage an investigation was made recording the breakdown potential for 20 consecutive start-ups. It was found that breakdown voltage could be consistently less than 30V. In the case of the T6 cathode, the anode cathode separation (0.5mm) considerably reduced the startup voltage. It was found that initiation was always possible so long as the voltage limit on the power supply was set higher than that of the cathode during operation at the respective mass flow rate, particularly with xenon. In this case the start-up voltage for the modified T6 operating with 0.5mgs^{-1} was consistently less than 12V.

D. Current Voltage Characteristics

Current voltage characteristics were obtained for operation of the T5 with argon over the flow range 0.05-mgs^{-1} to 1-mgs^{-1} and at 3.2A, 1.6A and 0.8A discharge current and with the T6 cathode at 10A, 20A, 25A and 30A with argon and 20A with xenon over the flow range 0.05 to 1-mgs^{-1} .

Typical voltage minimums were found in the T5 case at 0.65-mgs^{-1} , 0.68-mgs^{-1} and 0.82-mgs^{-1} at 3.2A, 1.6A and 0.8A respectively and are shown in Figure 15. This reduction in discharge voltage as flow rate is decreased is likely testament to an increasing ionization fraction within the orifice (and thus also downstream at the anode) which is driven by resistive dissipation and scales quadratically with current. This then corresponds to a lower cathode fall voltage required for the excitation of metastable states of argon to maintain the necessary plasma density at the anode to carry the discharge current. Higher currents therefore show lower voltage minimums. As mass flow rate is decreased further, maintenance of the plasma density at the anode can not be sustained by orifice dissipation alone which is likely compensated by an increase of excitation and ionization events within the cathode body (cathode fall), which increases the ionization fraction within the orifice, thus the cathode fall voltage begins to rise. Since there is no clear transition to plume mode but rather a smooth increase in operating voltage, it is anticipated that the majority of this voltage drop takes place within the cathode fall region between the emitter and the plasma sheath, rather than within the cathode anode gap (anode fall). Increase in anode fall can also be differentiated from cathode fall by the severe noise within the discharge and a transition region which was not present in this case.

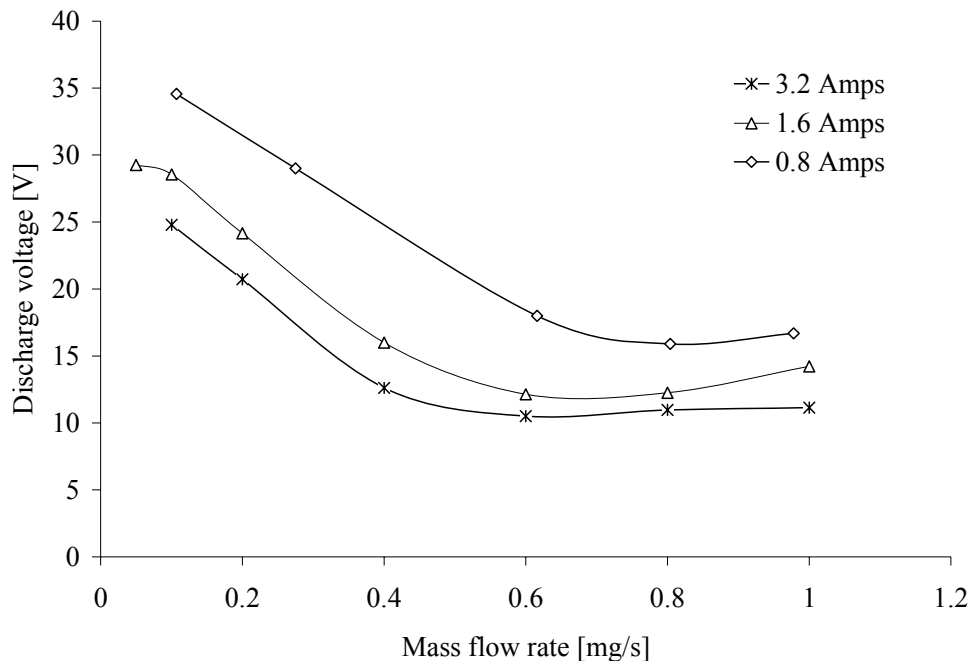


Figure 15 Current-voltage characteristics for the T5 cathode with argon

In the T5 cathode the fact that there is no sudden transition to plume mode but rather a gradual increased in voltage suggests that there is good electrical contact between the cathode, external plasma and the anode. This is most likely due to the large area available to the plasma on the inner face of the anode. This implies that the flat plate open keeper design may in fact significantly impede the flow of the plasma, and thus maintain a relatively high plasma pressure and density within the cathode-anode gap. For operation in terms of a thruster, this may be a sub-optimal configuration. It is also noted that during testing, arc root movement was visible around the exit of the anode orifice which was responsible for at least a 35° alteration of the thrust vector of the visible plume. This was only observable at high mass flow rates and low powers due to the intense brightness of the anode ring shown in figure 17. It is reasonable to suggest that this effect will be more pronounced at higher powers and currents, thus with higher ionization fractions and pinch forces.



Figure 16 T5 HCT during operation with argon at 70.3W (3.2A) at 21V with 0.05mgs⁻¹ (left) and 12.8W (0.8A) at 15V with 0.8mgs⁻¹ (right)

Plasma contact area was considered in the modified T6 cathode design primarily based on Equation (9), and maximizing the available contact area between the emitted plasma and the anode without significantly impeding the flow. This maximized thrust at reasonable discharge voltages while maintaining diffuse arc attachment. The very low operating voltages shown in Figure 16 are testament to this relationship. The discharge voltage in the T6 case only began to increase significantly (>15V) below 0.25mgs⁻¹ for even the highest discharge currents (30A) with the lowest possible flow rate being 0.045mgs⁻¹ at 28V with argon (Figure 18) and 0.040mgs⁻¹ at 42V with xenon. Above this flow rate there was little discernable difference in discharge voltage at all current conditions. Such low flow rates can not be obtained without suitable anode design and to the authors knowledge these are the lowest flow rates that a T6 cathode has ever been operated at while drawing such high discharge currents.

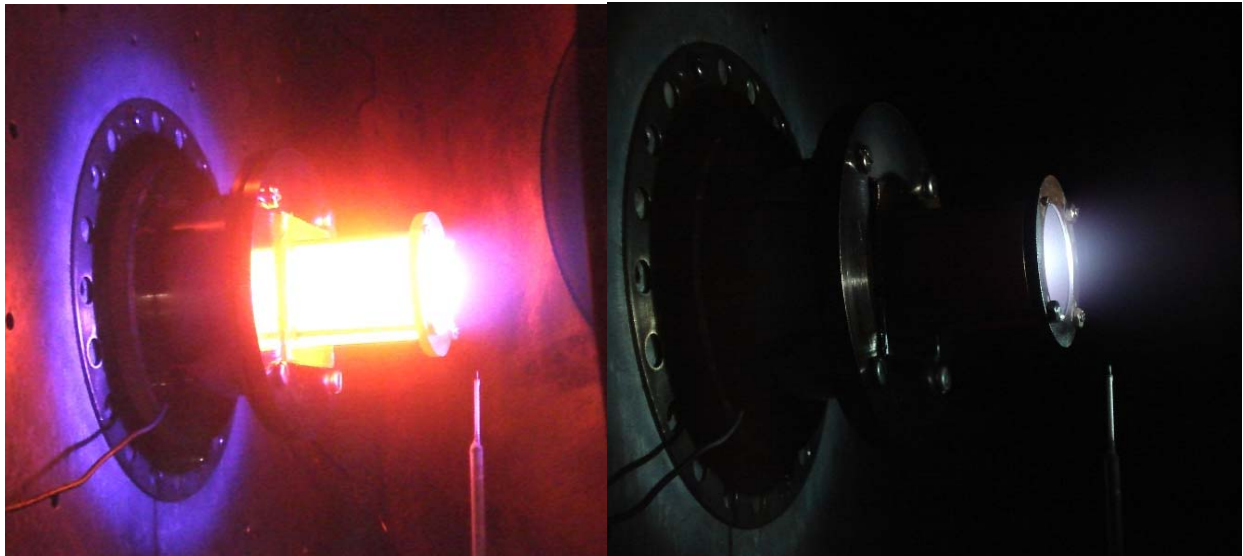


Figure 17 T6 cathode operating stably at 840W (30Amps) on argon at 0.045mgs⁻¹, 28.0V discharge voltage (left) T6 operating on xenon at 200W (25Amps) 0.5 mgs⁻¹ at 8.01V discharge voltage (right)

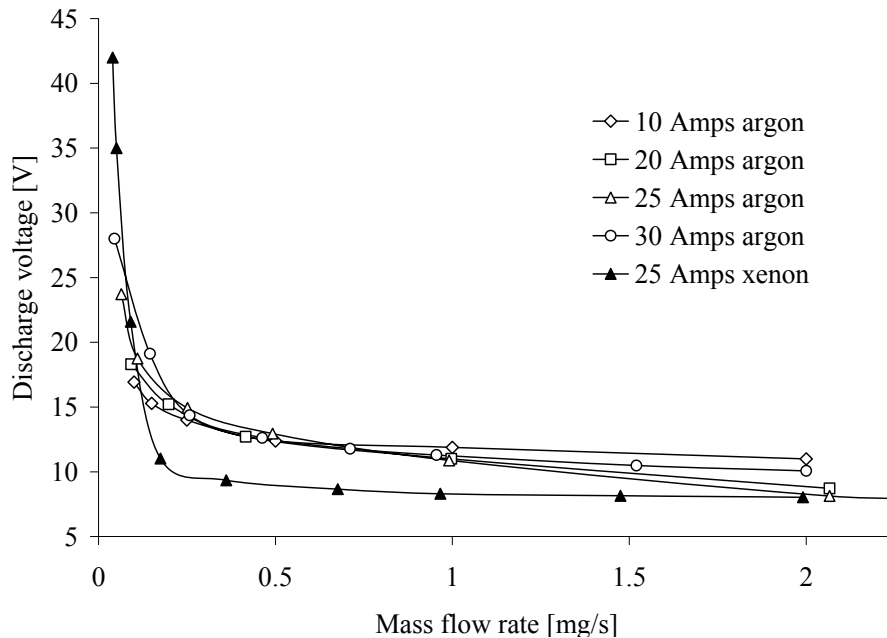


Figure 18 Current-voltage characteristics for the modified T6 cathode with argon and xenon

Operation with xenon gave consistently lower discharge voltages (testament to the lower primary ionization energy) and showed arguably the most impressive current voltage characteristics with the cathode delivering 25Amps at only 0.15mg/s^{-1} and 12V discharge voltage. Operation at higher mass flow rates gave reduction down to 8V. It should also be noted that there was also no transition to unstable modes of operation at very low mass flow rate in the modified T6 design. Discharge voltage is always stable and down to a critical point of mass flow rate then the cathode extinguishes, the reduction in back pressure encourages an increase in mass flow through the orifice and the cathode then enters into a pulsed mode of operation, continuously igniting and extinguishing until after a short time, the assembly temperature drops and the ignitions do not continue.

E. T5 Discharge Thrust Measurement

It should first be noted that to ensure the target was not being influenced by the plasma in which it is immersed, the target was biased +/- 30V and also directly grounded during high and low power operation. The thrust measurement system showed no sign of plasma interaction with the thrust balance affecting the thrust measurements. Results for the various current conditions for the T5 cathode are shown in Figure 19.

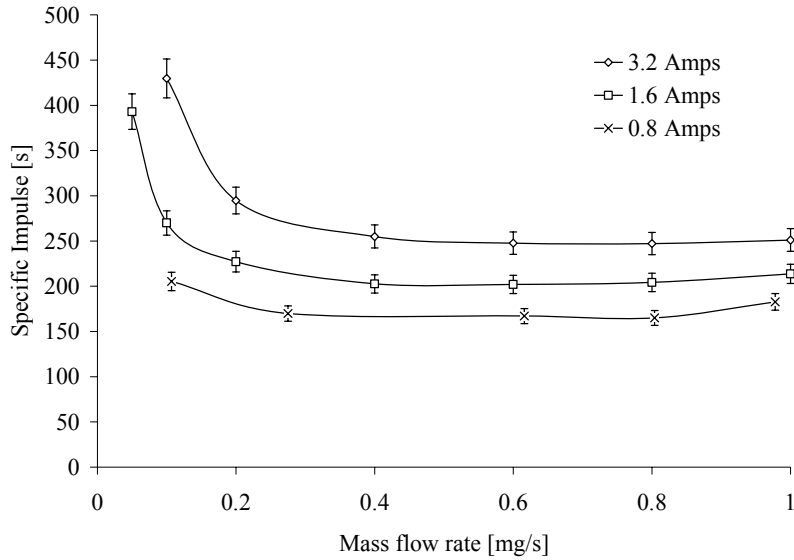


Figure 19 Specific impulse vs. mass flow rate for various throttle levels of the T5 cathode

Results show near monotonic dependence of specific impulse on discharge current with rapidly increasing performance below 0.4mg/s^{-1} for the 3.2A and 1.6A throttle settings with a less pronounced increase at 0.8A. Since a change in flow rate results in a change in operating voltage it is seen that specific impulse can be correlated with specific power of the flow ($\text{J}\cdot\text{mg}^{-1}$) and a product of the discharge current and operating voltage. Figure 20 shows the relationship between operating power and specific impulse and Figure 21 shows associated thrust efficiencies.

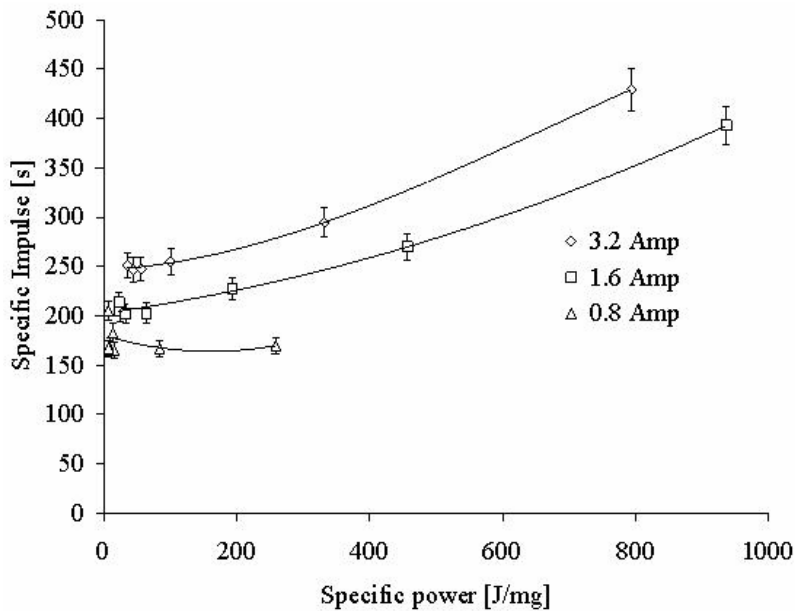


Figure 20 Dependence of specific impulse on specific power for the various current levels with argon

Operation at low powers ($<13\text{W}$) in the low current condition (0.8Amp) brings relatively high specific impulse of up to 165 seconds equal to performance in a resistojet mode (and at lower power), where cathode body temperatures are in the region of 1000°C . At the high current condition operation at powers of below 30W give specific impulse in the region of 250s. Further reduction in flow rate increases operating voltage and power invested

in the flow. This results in an increase in specific impulse however with declining thrust efficiency as convective and radiative losses begin to dominate.

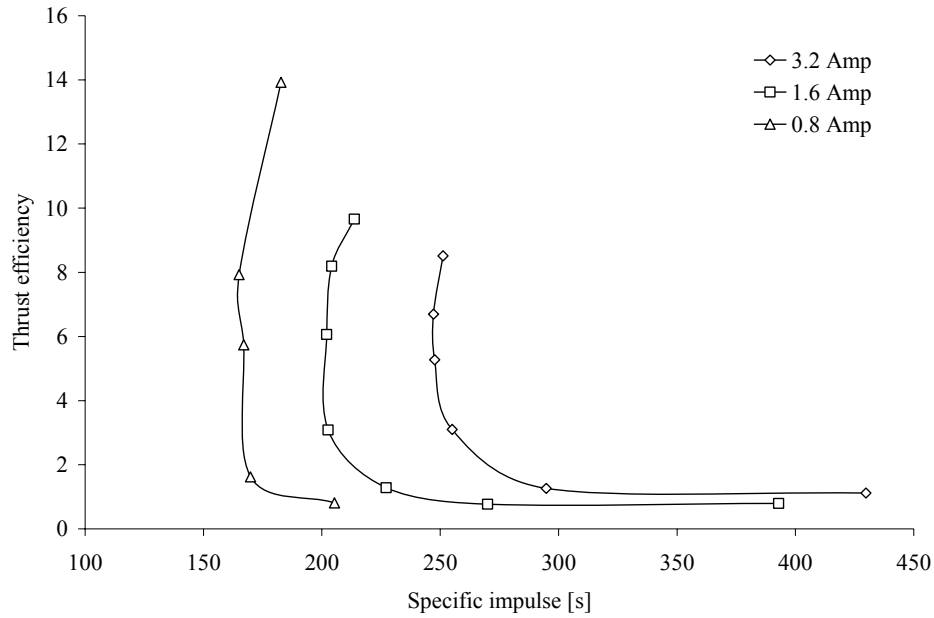


Figure 21 Associated thrust efficiencies in relation to specific impulse at various throttle conditions

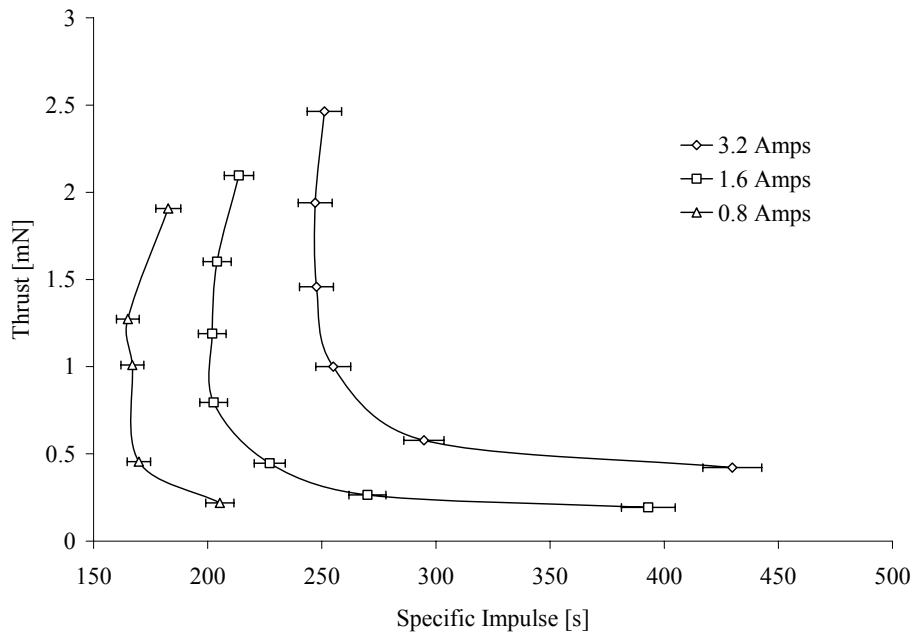


Figure 22 Thrust and specific impulse attained at various current conditions in the T5 cathode

Figure 22 shows thrust levels achievable with respect to specific impulse. The highest specific impulse of 429s was attained with the T5 cathode at 3.2A, with 1.1% thrust efficiency, 79W discharge power. Specific impulse can be traded for higher thrust to power ratios by increasing propellant flow rates or decreasing discharge current (however higher thrust efficiencies are obtained at higher discharge currents) generating thrust efficiencies of 14%

($200\mu\text{N/W}$) and specific impulse of 167s at 0.8Amps, and over 8% at the maximum rated current capacity of 3.2 Amps, with specific impulse $\sim 250\text{s}$ ($77\mu\text{N/W}$, 35W discharge power). Up to 2.4mN could be generated at higher currents, shown in Figure 22, with the maximum flow rate of 1-mgs^{-1} with specific impulse over 250s.

Respective discharge powers and performance can be seen in Figure 23 and highlights the ultimate power required to generate such performance.

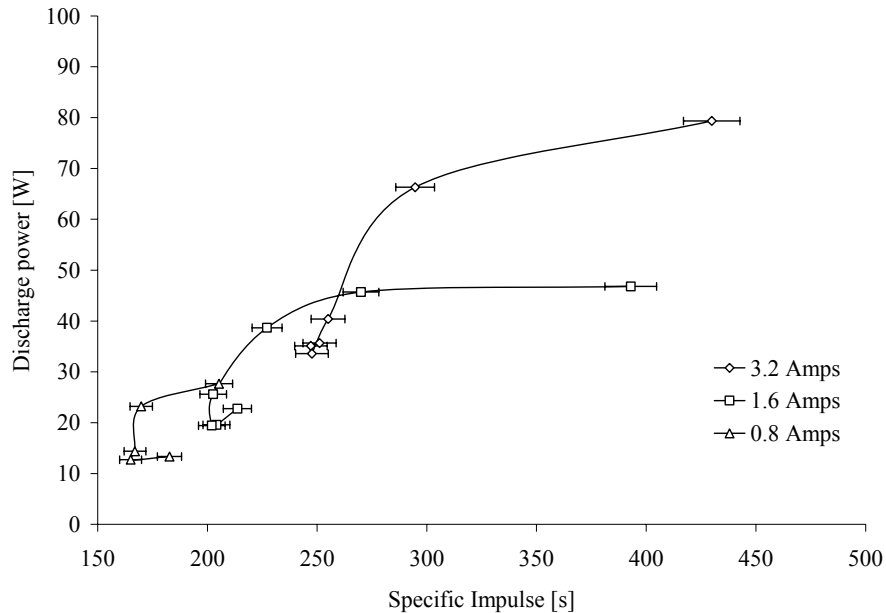


Figure 23 Performance variation with discharge power at various current conditions

F. T6 Discharge Thrust Measurement

Figure 24 shows that ultimately high specific impulse is dependant on discharge current since higher discharge currents are able to sustain operation at lower mass flow rates and higher powers. Operation with xenon also gives high specific impulse although only at the lowest flow rates. This is testament to the lower primary ionization energy of xenon, which enabled the cathode to operate at the lowest flow rate of 0.04mgs^{-1} .

Unlike the case of the T5 cathode, the T6 cathode shows relatively little improvement in specific impulse at higher currents indicating that resistive dissipation plays a much smaller role in thrust production, which is reasonable due to the large orifice of the T6 cathode. It is worth noting that at maximum current rated capacity, the current density in the T5 cathode is $65\text{A}\cdot\text{mm}^{-2}$ compared to the T6 cathode at $38\text{A}\cdot\text{mm}^{-2}$ which, assuming a an electrothermal acceleration mechanism, would suggest the reason for such larger relative changes in specific impulse of the T5 at higher currents.

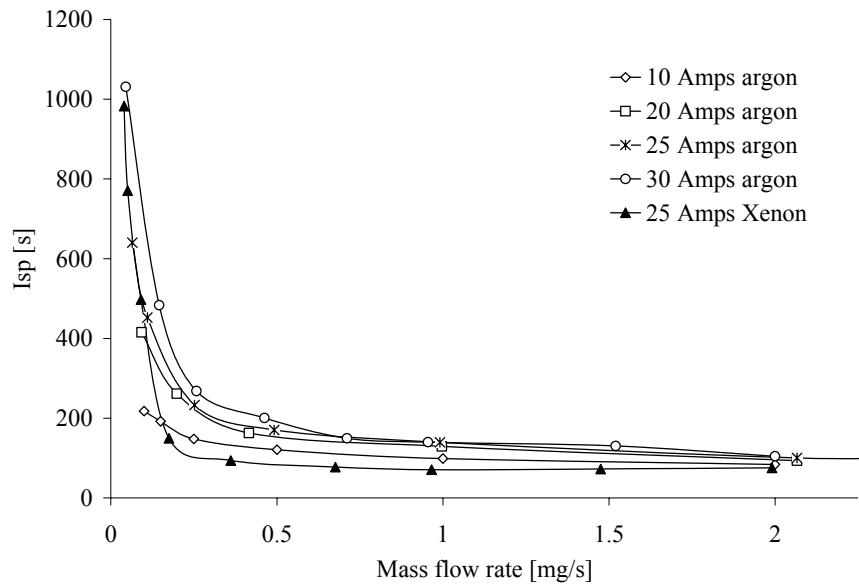


Figure 24 Specific impulse reached with the modified T6 hollow cathode at various current conditions and mass flow rates with xenon and argon

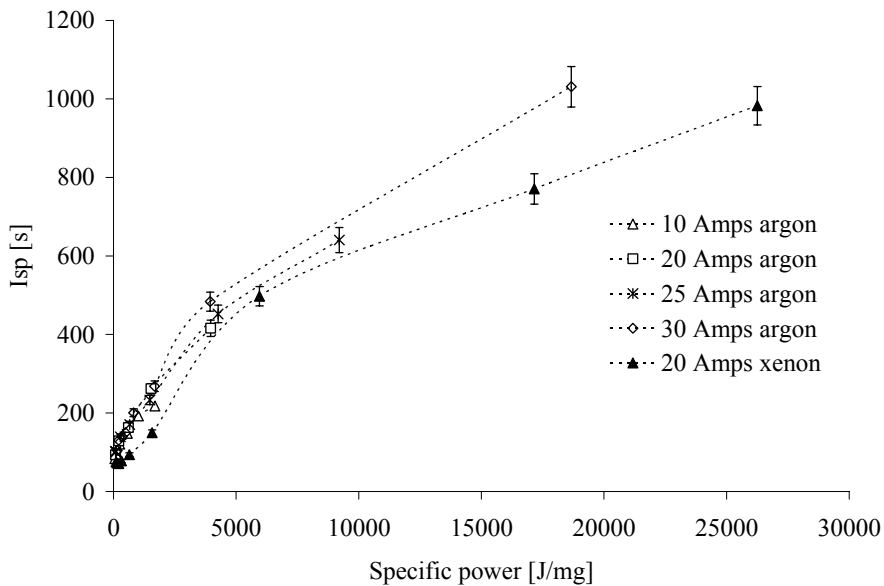


Figure 25 Relationship between specific impulse and specific power for the T6 at various current levels with xenon and argon

Figure 25 shows two distinct gradients in the relationship between specific power and specific impulse which differ substantially from the T5 results. For operation with argon, specific impulse is almost identical for low specific powers, however approaching $5000 \text{ J} \cdot \text{mg}^{-1}$ there is a change in gradient. It is postulated that this change in gradient is also a change in dominant thrust mechanism, with electromagnetic acceleration becoming the dominant accelerating mechanism, since flow rates above $5000 \text{ J} \cdot \text{mg}^{-1}$ are very low and would contribute an increasingly small degree of electrothermal thrust. This theory is strengthened when considering thrust level with respect to mass flow rate as in Figure 26.

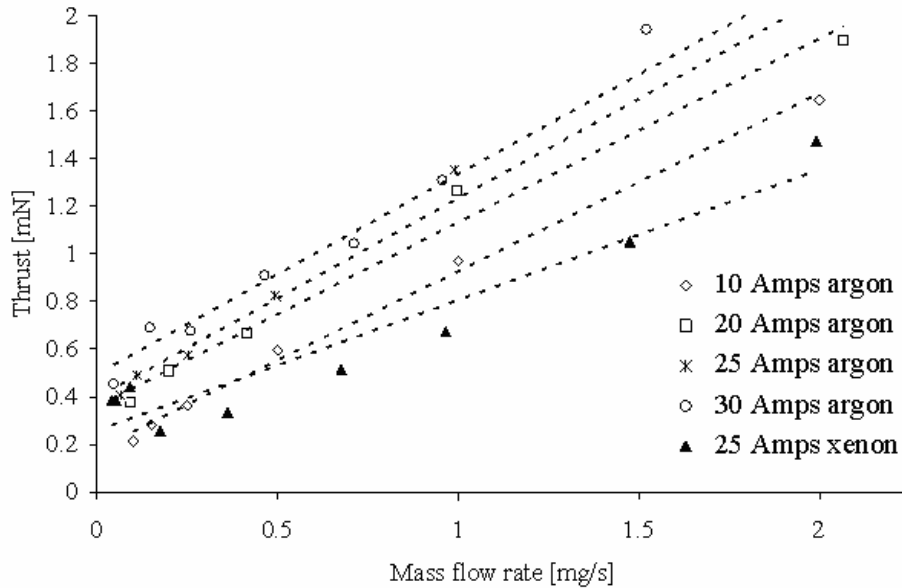


Figure 26 T6 thrust level with respect to mass flow rate at various current conditions with xenon and argon

It is clear that when extrapolating thrust level back to zero mass flow a remnant thrust production mechanism exists which is dependant on discharge current. The nature of this mechanism is made clear when overlaying the theoretical specific impulse obtainable by electromagnetic blowing force with the results obtained from the T6 cathode, shown in Figure 27.

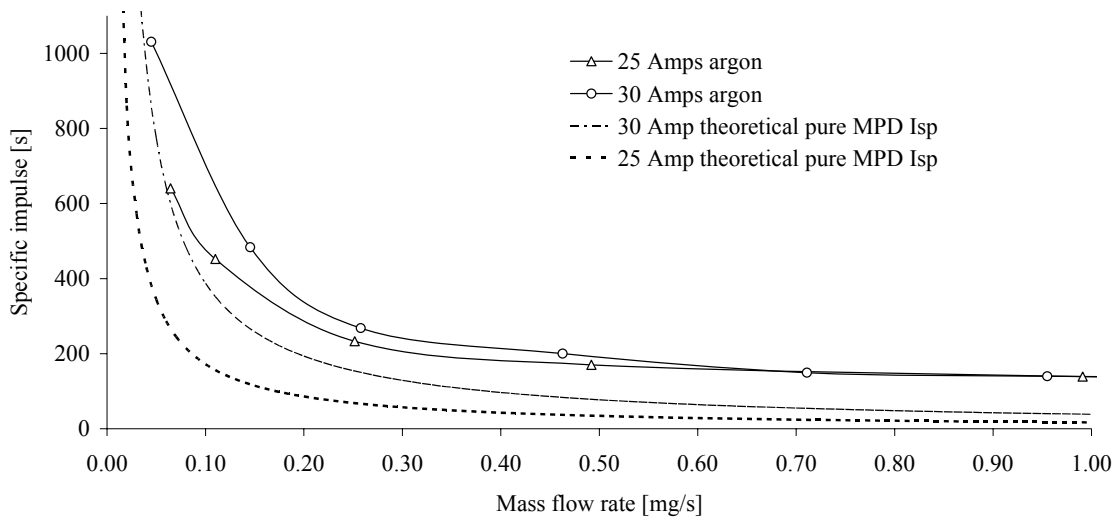


Figure 27 Experimental and theoretical specific impulse obtained from operation at 25 and 30 Amps with the modified T6 cathode with argon

The result shows a high likelihood that the increased specific impulse found at low and minimum mass flow rate is almost entirely due to MPD forces acting on the plasma. If the theoretical values are subtracted from those found in experiment consistent values of specific impulse between 200 and 300 seconds remain, explicable by the additional thermal thrust production mechanism and similar to values found in the T5 case. Since large discharge currents are required to produce a relatively small blowing force, thrust to power ratios are far below 1% in all but the 30A case for high specific impulse.

VI. Conclusion

Discharge power characteristics of the T5 cathode would suggest that the application of multiple hollow cathode thrusters for all-electric spacecraft would be well within the resource constraints of larger spacecraft which also carry primary electric propulsion systems. For smaller, more resource limited spacecraft low power hollow cathode thrusters may provide a basis to complement to existing architectures or as stand-alone thrusters. T5 hollow cathode characterization has provided baseline performances for a low power plasma propulsion device. Given that the anode geometry is far from suitable as a flat plate orifice, significant improvements in performance should be possible. The use of an enclosed anode similar to the modified T6 design will reduce operating voltage and improve thrust efficiency. Operation at higher currents has shown to be beneficial for high thrust to power ratios and useful thrust levels. Future work should be aimed at both maintaining low discharge voltages at higher current levels and higher thrust to power ratios, and improving high end performance at much higher specific powers. Such development will enable a thruster which can operate over a very large range of specific impulse and thrust.

The discharge characteristics of the T5 cathode are shown to be promising at least after several tens of hours of testing. With sufficient preheating time, no strike voltage was required for starting and the cathode initiated readily with less than 28V from the anode supply. This indicates that it could also be possible, at least in early cathode life, to start a discharge from a 28V bus with no power conditioning. Discharge powers suggest that a hollow cathode thruster based on the T5 cathode will make a suitable addition to microsatellite propulsion systems. The ability to avoid the use of power electronics and easily integrate hollow cathodes with conventional low cost cold gas (xenon, argon, nitrogen) architectures also advocate the simplicity of such a propulsion system. Operation in cold gas and resistojet modes highlights that redundancy in such a propulsion system is possible; however optimization requires a major redesign of the thruster. The results show that in certain operating conditions the T5 HCT is capable of impressive performance as an electro-thermal thruster with argon, explicable only by the heating of propellant up to many thousands of Kelvin (a conservative estimate based on possible overestimation of thrust), with thrust to power ratios between 30-250W/mN. The low current of the T5 means that the cathode must work as an electrothermal thruster and as such it would seem that resistive dissipation within the orifice is the specific impulse driver at any particular flow rate. Alternatively the T5 resistojet mode offers a much lower power to thrust ratio which may be beneficial for example when considering maneuvering times on initial de-spin of spacecraft on orbit insertion.

The exact thrust mechanisms of the T6 hollow cathode have been debated for some time. Our results indicate that for high specific impulse the hollow cathode operates as a low power MPD thruster. Due to the relatively low currents, electron convective and radiative losses dominate performance and thus give poor thrust efficiencies. Operation at elevated currents is likely to significantly improve performance and thrust efficiency; although this will be well beyond the rated current capacity for the T6 cathode. Subtracting the thrust production by electromagnetic acceleration would indicate that while electrothermal acceleration does play a role in T6 thrust production, it does not increase significantly as mass flow is decreased. This suggests that either electron temperature does not increase significantly at lower flow rates or that the energy equipartition between electrons-ions and electron-neutrals remains too low for any substantial increase in heat transfer.

The low voltages obtained in the modified T6 design highlight the importance of plasma anode interaction and cathode and keeper design. Previously keeper design has been considered relatively insignificant; however as has been shown optimized keeper design is imperative for hollow cathode thrusters, but also for neutralizers for Hall thrusters, ion engines and plasma contactors for minimization of discharge voltage and propellant loss. It should also be noted that the artificial backpressure becomes important at low mass flow rates are decreased as a means to maintain higher internal pressures. The T6 design also highlights the effect of anode cathode spacing on ignition voltage and potential for further optimization. The T5 and T6 in their current form could operate from a regulated 28V bus on large and small spacecraft without the need for high strike voltages.

At this time no investigation has been possible into the effect of elastic and non-elastic collisions with the target. This effect may be significant due to the planar geometry of the target. The effect is visible in operation of the cold gas thruster. The theoretical specific impulse for this type of operation should be around 50s with argon, the apparent specific impulse is around 80s. It should therefore be noted that this overestimation of thrust and thus specific impulse will also be consistent in the results for operation in a discharge mode at this preliminary stage. Future work will therefore be aimed at designing a pendulum target which is able to limit the effect of elastic collisions by controlling particle paths.

Acknowledgments

The author would like to dedicate this work to the late David Fearn; a master of his field and a gentleman whom without, this work would not be possible. His continued dedication to his field over the last 50-years has brought about revolutions in electric propulsion, and to those who knew him he was truly one of the greats. His knowledge, humor and company will be sorely missed.

References

- ¹ Gray, H L, "*Development of ion propulsion systems*", *GEC Rev*, 12, 3, 154-168, 1997.
- ² Wallace, N C and Feam, D G, "*The design and performance of the T6 ion thruster*", AIAA Paper 98-3342, 1998.
- ³ Fearn, D, Singfield, A, Wallace, N, Gab-, S and Harris, P, "*The operation of ion thruster hollow cathodes using rare gas propellants*", AIAA Paper 90-2584, 1990.
- ⁴ Latham, P M, Martin, A R and Bond, A, "*Design, manufacture and performance of the UK-25 engineering model thruster*", AIAA Paper 90-2541, 1990.
- ⁵ Harris, P T and Gair, S, "*A review of the cathode construction for the RAE 10/25 mN thruster*", IEPC Paper 88-078, 1988.
- ⁶ Philip, C M and Fearn, D G, "*Recent hollow cathode investigations at the Royal Aircraft Establishment*", AIAA paper 73-1137, (1973); AIAA J, 12, 10, 1319-25, 1974.
- ⁷ Fearn, D G, "*The operation of hollow cathodes under conditions suitable for ion beam neutralization*", Proc Conf on Electric Propulsion of Space Vehicles, Culham Laboratory, UK, (April 1973). Inst of Electrical Engineers Conference Publication 100, pp 146-150, 1973.
- ⁸ S. Pottinger, P. Gessini, D. Webb, R. Intini Marques and S. B. Gabriel, "*Electric Propulsion Research at the University of Southampton*", Journal of the British Interplanetary Society, Vol. 59, No. 5, May 2006.
- ⁹ P. Gessini, S. B. Gabriel and D. G. Fearn, "*Thrust Characterization of a T6 Hollow Cathode*", IEPC Paper 05-257, 29th International Electric Propulsion Conference, Princeton, NJ, October-November 2005.
- ¹⁰ P. Gessini, S. B. Gabriel and D. G. Fearn, "*The T6 Hollow Cathode as a Microthruster*", AIAA Paper 2005-4078, 41st AIAA/ASME/SAE/ASEE Joint Propulsion Conference & Exhibit, Tucson, AZ, July 2005.

-
- ¹¹ Rayman, Marc D. and David H. Lehman, "NASA's First New Millennium Deep-Space Technology Validation Flight," Second IAA International Conference on Low-Cost Planetary Missions, Laurel, MD, April 16-19, 1996, IAAL-0502.
- ¹² P. Bodin, S. Berge, M. Bjork, A. Edfors, J. Kugelberg and P. Rathsman "The SMART-1 Attitude and Orbit Control System: Flight Results from the First Mission Phase", AIAA-2004-5244 AIAA Guidance, Navigation, and Control Conference and Exhibit, Providence, Rhode Island, Aug. 16-19, 2004
- ¹³ H. Kuninaka, Y. Shimizu, T. Yamada, I. Funaki and K. Nishiyama, "Flight Report During Two Years on HAYABUSA Explorer Propelled by Microwave Discharge Ion Engines", AIAA-2005-3673, 41st AIAA/ASME/SAE/ASEE Joint Propulsion Conference and Exhibit, Tucson, Arizona, July 10-13, 2005
- ¹⁴ Rayman, M. D., Frascettia, T. C., Raymond, C. A., Russell C. T., "Preparing for the Dawn Mission so Vesta and Ceres", IAC-05-A3.5.B.011, 56th International Astronautical Congress, 17 - 21 October 2005, Fukuoka, Japan,
- ¹⁵ Moerel, J., Marée, T., Bombelli, V., Simon D., "Economic Benefits of the Use of Non-Toxic Mono-Propellants for Spacecraft Applications", AIAA-2003-4783 39th AIAA/ASME/SAE/ASEE Joint Propulsion Conference and Exhibit, Huntsville, Alabama, July 20-23, 2003
- ¹⁶ Jankovsky, R. S., Sankovic, J. M., Oleson, S., "Performance of a FAKEL K10K resistojet", AIAA-1997-3059 AIAA/ASME/SAE/ASEE Joint Propulsion Conference and Exhibit, 33rd, Seattle, WA, July 6-9, 1997
- ¹⁷ Coxhill, I., Gibbon, D., "A Xenon Resistojet Propulsion System for Microsatellites", AIAA-2005-4260 41st AIAA/ASME/SAE/ASEE Joint Propulsion Conference and Exhibit, Tucson, Arizona, July 10-13, 2005
- ¹⁸ Coletti, M., Grubisic, A. Wallace, N., Wells, N., "European Student Moon Orbiter Solar Electric Propulsion Subsystem Architecture – An All-Electric Spacecraft" IEPC-2007-111 30th International Electric Propulsion Conference, Florence, Italy September 17-20, 2007 M.
- ¹⁹ Walker, R., "The SIMONE Mission: low-cost Exploration of the Diverse NEO Population via Rendezvous with Microsatellites", IAC-03-Q.5.05 54th International Astronautical Congress of the International Astronautical Federation, the International Academy of Astronautics, and the International Institute of Space Law, Bremen, , Sep. 29-3, 2003
- ²⁰ Inter-Agency Space Debris Coordination Committee, Space Debris Mitigation Guidelines, IADC 02-01 (2002)
- ²¹ Baker, A. M., Da-Silva-Curiel A, Schaffner, J., Sweeting, M. "Advanced Low Cost Propulsion Concepts for Small Satellites Beyond LEO", IAC Paper No. 04-IAF-S.1.08 (2004).
- ²² Manzella, D. H.; Curran, F. M.; and Zube, D. M., "Preliminary Plume Characteristics of an Arcjet Thruster," AIAA Paper No. 90- 2645 (1990).
- ²³ Mueller J., "Thruster Options for Microspacecraft" from "Micropropulsion for Small Spacecraft" Volume 187 Progress in Astronautics and Aeronautics.
- ²⁴ Jack, T M, "The characterization of the STRV small satellite charge alleviation cathode", Proc Third Intemat Workshop on Transient Hollow Cathode Discharge Phenomena, Paris, 14-16 September 1994.

-
- ²⁵ Crofton, M.W., “*Evaluation of the United Kingdom Ion Thruster*” J. Spacecraft and Rockets, Vol. 33, No. 5, 1996, pp. 739-747.
- ²⁶ Cronin, J.L., “*Modern Dispenser Cathodes*” IEEE Proc. 128, 19–32 (1981).
- ²⁷ Martin, R. A., “*Atomic Excitation Processes in the Discharge of Rare Gas Ion-Engines*,” J. Phys. B Atom. Molec. Phys., Vol. 7, No. 10 (1974).
- ²⁸ Crofton, M., Boyd, I. D., “*Plume Measurement and Modelling Results for a Hollow Cathode Micro-Thruster*,” AIAA Paper No. 2001-3795 (2001).
- ²⁹ Sarver-Verhey, T. R., “*28,000 Hour Xenon Hollow Cathode Life Test Results*,” IEPC Paper No. 97-168 (1997).
- ³⁰ Rawlin, V. K., “*A 13,000 Hour Test of a Mercury Hollow Cathode*,” NASA TM X-2785 (1973).
- ³¹ Sarver-Verhey, T.R., “*Extended Test of a Xenon Hollow Cathode for a Space Plasma Contactor*,” NASA CR–195402 (1994).
- ³² Polk J.E., Grubisic A. N., Goebel D., “*Emitter Temperature Distributions in the NSTAR Discharge Hollow Cathode*” AIAA-2005-4398, 41st AIAA/ASME/SAE/ASEE Joint Propulsion Conference, Tucson, AZ, 2005
- ³³ Grubisic A.N., “*Temperature Characterization and Optimization of an NSTAR Discharge Cathode for the Deep Space-1 Gridded Ion-Engine*” Masters Thesis, International Space University, Strasbourg, France 2005
- ³⁴ Rehn, L. and Kaufman, H.R., “*Correlation of Inert Gas Hollow Cathode Performance*,” AIAA Paper No. 78-707 (1978).
- ³⁵ Sahli, A., Turchi, P.J., “*Low Power Plasma Thruster Based on a Hollow Cathode Discharge*”, AIAA Paper No. 94-3126 (1994).
- ³⁶ Williams, G., Smith, T., Domonkos, M., Shand, K., and Gallimore, A., “*Laser Induced Fluorescence Characterization of Ions Emitted from a Hollow Cathode*,” AIAA Paper No. 99-2862 (1999).
- ³⁷ Domonkos, M. T., Gallimore, A. D., and Patterson, M. J., “*An Evaluation of Hollow Cathode Scaling to Very Low-power and Flow Rate*,” IEPC Paper No. 97-189 (1997).
- ³⁸ Katz, I. and Patterson, M. J., “*Optimizing Plasma Contactors for Electrodynamic Tether Missions*,” Tether Technology Interchange, Huntsville, AL, Sept. 1997.
- ³⁹ Mikellides I., Katz ., Goebel D. M., and Polk J. E., , “*Theoretical Model of a Hollow Cathode Plasma for the Assessment of Inert and Keeper Lifetimes*”, AIAA Paper No. 2005-4234 (2005).
- ⁴⁰ C. H. Edwards “*Discharge Characteristics and Instabilities in the UK-25 Ion Thruster Operating on Inert Gas Propellants*” PhD. Thesis, University of Southampton, 1997.